Hindawi Publishing Corporation
International Journal of Inorganic Chemistry
Volume 2010, Article ID 975756, 7 pages
doi:10.1155/2010/975756

Research Article

Reaction of the Anticancer Organometallic Ruthenium Compound, $[(\eta^6\text{-}p\text{-Cymene})\text{Ru(ATSC)Cl}]PF_6$ with Human Serum Albumin

Floyd A. Beckford

Science Division, Lyon College, 2300 Highland Road, Batesville, AR 72501, USA

Correspondence should be addressed to Floyd A. Beckford, fbeckford@lyon.edu

Received 8 September 2009; Accepted 6 November 2009

Academic Editor: Stephen Ralph

The reaction of $[(\eta^6\text{-}p\text{-cymene})\text{Ru(ATSC)Cl}]PF_6$ (ATSC = 9-anthraldehyde thiosemicarbazone) with human serum albumin was investigated at different temperatures using fluorescence and infrared spectrophotometry. The binding constant, K, for the reaction was determined using a number of different methods. Using a modified Stern-Volmer equation, K was determined to be $9.09 \times 10^4, 12.1 \times 10^4$, and $13.1 \times 10^4\,M^{-1}$ at 293 K, 298 K, and 308 K, respectively. A thermodynamic analysis showed that the reaction is spontaneous with ΔG being negative. The enthalpy of reaction $\Delta H = 16.5\,kJ\,mol^{-1}$ and the entropy of reaction $\Delta S = 152\,Jmol^{-1}K^{-1}$. The values of ΔH and ΔS suggest that hydrophobic forces are dominant in the mode of interaction and that the process is mostly entropy driven.

1. Introduction

Ruthenium complexes of various types are actively studied as metallodrugs as they are believed to have low toxicity and good selectivity for tumors [1]. Very recently, two ruthenium-(III) complexes have also successfully completed phase I clinical trials, namely, NAMI-A [2–5] (NAMI-A, (ImH)[*trans*-Ru(III)Cl_4Im(Me_2SO)]; Im = imidazole), and KP1019, indazolium *trans*-[tetrachlorobis(1*H*-indazole)ruthenate(III)] [6–8]. Organometallic compounds exhibit different ligand exchange kinetics in solution to coordination complexes, as well as novel structural motifs and organometallic ruthenium(II)-arene complexes (of the type $[(\eta^6\text{-arene})\text{Ru(LL)Cl}]^+$, LL = ligand) are also currently attracting increasing interest as anticancer compounds [9, 10]. Complexes such as $[(\text{arene})\text{Ru(en)Cl}]^+$ are even active in cisplatin-resistant cell lines [9]. While it is believed that DNA is a primary target for these complexes, since DNA replication is integral to the progression of these diseases, there is also the recognition that the observed biological activity is not always related to their DNA-binding ability. As a consequence, investigations that seek to examine the interaction with serum and cellular proteins are beginning to be undertaken [11–14].

As the principal extracellular protein of the circulatory system, human serum albumin (HSA), serves as the major transporter of drugs as well as endogenous compounds such as fatty acids since these compounds can bind reversibly to the HSA [15, 16]. It has been shown that the distribution, free concentration, and the metabolism of various drugs can be significantly altered as a result of their binding to HSA. HSA also often increases the apparent solubility of hydrophobic drugs in plasma. Since HSA serves as a transport carrier for drugs, it is important to study the interactions of potential drugs with this protein. Knowledge of interaction mechanisms between drugs and plasma proteins is of crucial importance to the understanding of the pharmacodynamics and pharmacokinetics of a drug or drug prospect.

Many protein interaction assays are designed around the changes in the intensity and or the position of major chromophores of the protein on conjugation with another substance. Fluorescence quenching and FTIR are powerful tools and are important methods to study the interaction of small molecules with proteins. Both are relatively easy to use and are capable of sensing small concentrations of the

reactants. In addition both techniques are capable of detecting changes in the environment of the protein, in particular changes in tryptophan fluorescence or changes in the amide I band absorbance caused by changes to the protein structure. This communication describes the nature of the interaction between an organometallic ruthenium complex, [(η^6-*p*-cymene)Ru(anthraldehyde thiosemicarbazone)Cl]PF_6, **1** (Figure 1) and HSA.

2. Experimental

Analytical or reagent grade chemicals were used throughout. All the chemicals including solvents were obtained from Sigma-Aldrich (St. Louis, MO, USA) or other commercial vendors and used as received. The metal complex was synthesized as described earlier [17]. The doubly purified water used in all experiment was from a Milli-Q (Millipore Inc) system. Solutions of HSA were prepared in Tris buffer (50 mM Tris, pH 7.40, 100 mM NaCl) and stored in the dark at 4°C. The protein concentration was determined spectrophotometrically using the molar absorptivity of 36 000 M^{-1} cm^{-1} at 280 nm [18]. Concentrated solutions of the complex were made up in a 70% mixture of DMSO and Tris buffer. Fluorescence spectra were recorded on a Varian Cary Eclipse spectrophotometer. For the fluorescence titration experiments, a 3.0 cm^3 solution of HSA (3 μM) was placed in a quartz cuvette and titrated with various amounts of a concentrated solution of the complex producing the solutions with varied mole ratios of complex to HSA. The complex concentration ranged from 3 to 30 μM. After each addition the solution was mixed for 30 seconds and allowed to sit at the appropriate temperature for 5 minutes before measurement. The fluorescence spectra of the solutions were obtained by exciting at 295 nm and measuring the emission spectra from 300 to 500 nm using 5 nm slits. Temperature was controlled using a single-cell Peltier accessory. Infrared (IR) spectra in the range 1200–2000 cm^{-1} were obtained using the ATR accessory (with a diamond crystal) on a Nicolet 6700 FTIR spectrophotometer equipped with a DTGS KBr detector and a KBr beam splitter. The infrared spectra of HSA, HSA plus the complex (1 : 1 molar ratio), and the complex alone were recorded. The HSA-complex solutions were incubated for 24 hours prior to measurement. The absorbance of the buffer was subtracted from the spectra of the solutions. Then difference spectra were calculated using the instrument's software package.

3. Results and Discussion

*3.1. Interaction of **1** with HSA.* [(η^6-cymene)Ru(ATSC)Cl]PF_6, **1**, (9-ATSC = anthraldehyde thiosemicarbazone) is an anticancer compound shown to be effective against breast (MCF-7 and MDA-MB-231) and colon HCT-116 and HT 29) cell lines at low micromolar concentrations [17]. The reaction of **1** with HSA was initially characterized by fluorescence spectrophotometry. Fluorimetry is a simple yet effective method for investigating the strength and mode of binding of small molecules to HSA. HSA has a well-known structure

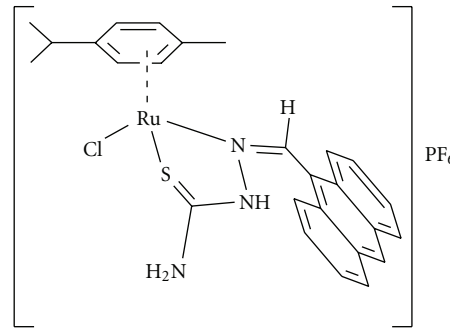

Figure 1: Structure of [(η^6-*p*-cymene)Ru(anthraldehyde thiosemicarbazone)Cl]PF_6, **1**.

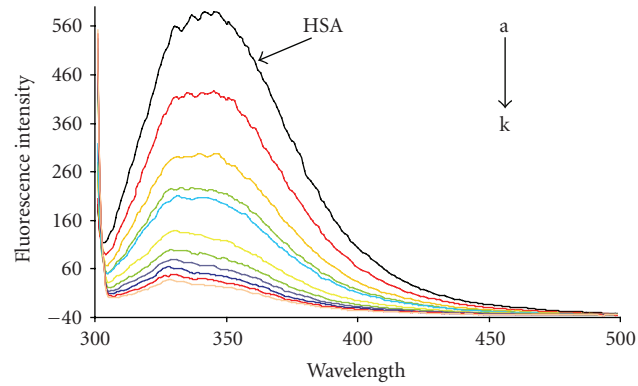

Figure 2: Fluorescence emission of HSA in the presence of increasing amounts of **1**. [HSA] = 3.0 μM; [Ru] =(a) 0, (b) 3.0, (c) 6.0, (d) 9.0, (e) 12.0, (f) 15.0, (g) 18.0, (h) 21.0, (i) 24.0, (j) 27.0, and (k) 30.0 μM. Temperature = 20°C.

consisting of a single polypeptide chain. Of the amino acid residues in the chain, the single tryptophan (Trp 214) is responsible for the majority of the intrinsic fluorescence of the protein. HSA has a strong fluorescence emission with a peak near 350 nm upon excitation at 295 nm. This emission is sensitive to the changes in the local environment of the tryptophan and so can be attenuated by binding of a small molecule at or near this residue.

Figure 2 shows that the addition of the complex to HSA results in a significant reduction in the fluorescence intensity with a blue shift to 330 nm ($\Delta\lambda$ = 17 nm). These changes indicate that the conformation of the protein is affected by binding to the metal complex. The wavelength shift is likely due to the environment of the tryptophan becoming more nonpolar [19].

3.2. Quantitative Analysis of Titration Data

3.2.1. Nonlinear Analysis. A quantitative assessment of the fluorescence data to determine the strength and possible mode of binding can be made by treating the data using a number of different methods. Fluorescence quenching can occur by what is commonly described as a static mechanism

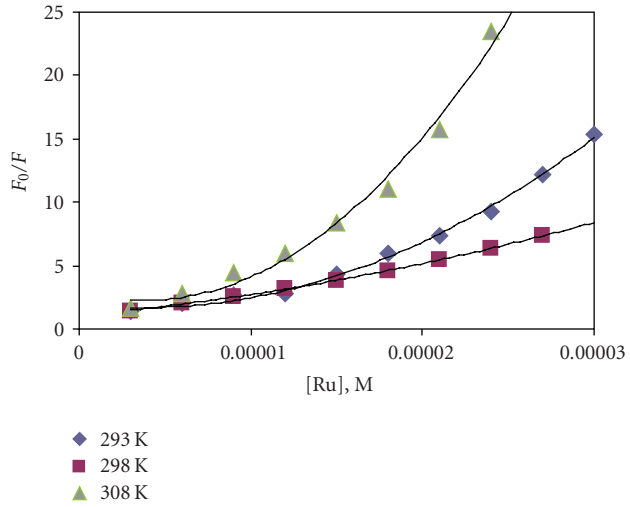

FIGURE 3: Stern-Volmer plots for the quenching of HSA fluorescence by **1** at different temperatures.

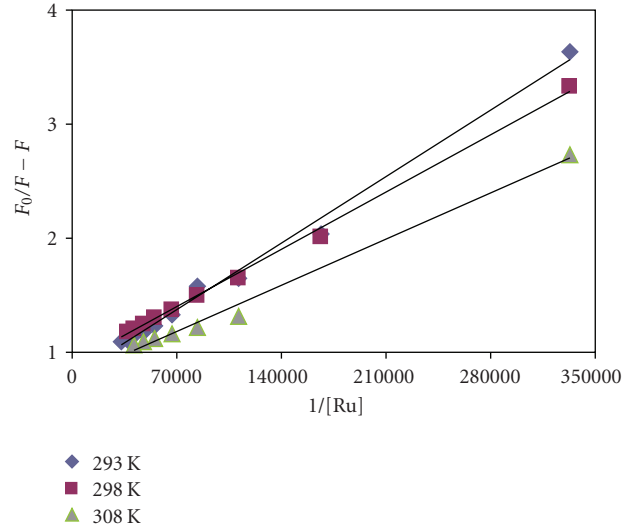

FIGURE 4: Plot of the modified Stern-Volmer equation $F0/(F0 - F)$ versus 1[Ru].

or a dynamic mechanism. Quantitatively, these can be described by the Stern-Volmer equation

$$\frac{F_0}{F} = 1 + K_{SV}[\text{Ru}] = 1 + k_q \tau_0 [\text{Ru}], \quad (1)$$

where F_0 and F are the HSA fluorescence intensities in the absence and presence of **1** (**1** represented as Ru) and K_{SV} is the Stern-Volmer quenching constant. As Figure 3 shows, a plot of F_0/F versus [Ru] is not completely linear as expected since there is obvious positive deviation at higher complex concentrations. There are two common explanations for this deviation. First the HSA can be quenched via both of the common quenching mechanisms operating simultaneously.

Alternatively there might be more than one independent binding site on the HSA and they are not all accessible to the complex. When both static and dynamic quenching is occurring, the quenching data can be treated using the following equation:

$$\frac{F_0}{F} = (1 + K_S[\text{Ru}])(1 + K_D[\text{Ru}]) \quad (2)$$

which on manipulation leads to

$$\frac{F_0}{F} = 1 + K_1[\text{Ru}] + K_2[\text{Ru}]^2, \quad (3)$$

where $K_1 = K_S + K_D$ and $K_2 = K_S K_D$ (K_S and K_D are the static and dynamic quenching constants). The second-order nature of (3) is reflected in the curvature of the Stern-Volmer plot. An attempt was made to fit the experimental data to (3) using the Solver add-in within Microsoft Excel. At 20°C, the quadratic equation could not be solved as imaginary numbers would result. However at 25°C and 35°C, values of 186,987 and 5,321 M^{-1} and 604,962 and 5,785 M^{-1}, respectively, were obtained corresponding to values for K_D and K_S. Which value corresponds to which constant can be deduce by calculating the second-order rate constant, k_q, from the Stern-Volmer equation. If K_D is 186,987 M^{-1}, k_q is calculated to be 1.87×10^{13} M^{-1} s^{-1}, assuming $\tau_0 = 10$ ns [20] for the HSA. At 35°C k_q was 6.04×10^{13} $M^{-1}s^{-1}$. These values are much greater than the maximum collisional quenching constant of 2.0×10^{10} M^{-1} s^{-1} [21]. So the values of 186,987 and 604,962 are assigned to K_S meaning that that static contribution to the quenching is dominant.

3.2.2. Modified Stern-Volmer Analysis. Assuming that the quenching process is predominantly static (at the lower concentrations of **1**), the binding constant for the reaction can be obtained from a modified Stern-Volmer (MSV) analysis. This involves treating the data using

$$\frac{F_0}{F_0 - F} = \frac{1}{f} \cdot \frac{1}{K[\text{Ru}]} + \frac{1}{f}, \quad (4)$$

where f = fraction of the fluorophore that is initially accessible to the metal complex and K is the effective quenching constant for the accessible fluorophore which can be taken as a binding constant (assuming the decrease in fluorescence comes from the interaction of the HSA with **1**. Figure 4 shows the plot of $F_0/(F_0 - F)$ as a function of 1/[Ru]. The value of the binding constant (given in Table 1) was found from the ratio of the intercept to the slope. The mean fractional accessibility over the temperature range studied is 1.2. This implies that there might be more than one binding site for **1** and that the molecular environment of the tryptophan is easily accessible to the complex, at least initially.

3.2.3. Scatchard Analysis. To further examine the strength of binding, the Scatchard method was used to analyze the data. This method has its limitations (particularly since the transformation distorts experimental error) but it remains a common method for analysis and presentation of binding

Table 1: Binding constants for the interaction of [(cymene)Ru(ATSC)Cl]PF_6 with the HSA.

	Modified Stern-Volmer		Scatchard		Lineweaver-Burk	
Temperature (K)	K (10^4 M^{-1}) (f)	R^2	K (10^4 M^{-1}) (n)	R^2	K (10^4 M^{-1})	R^2
293	9.09 ± 0.48 (1.32)	0.993	11.5 ± 0.3 (1.22)	0.997	9.15 ± 0.49	0.993
298	12.1 ± 0.3 (1.15)	0.997	12.7 ± 0.5 (1.13)	0.990	12.2 ± 0.4	0.997
308	13.1 ± 0.8 (1.33)	0.992	14.7 ± 1.8 (1.27)	0.988	13.3 ± 1.1	0.982

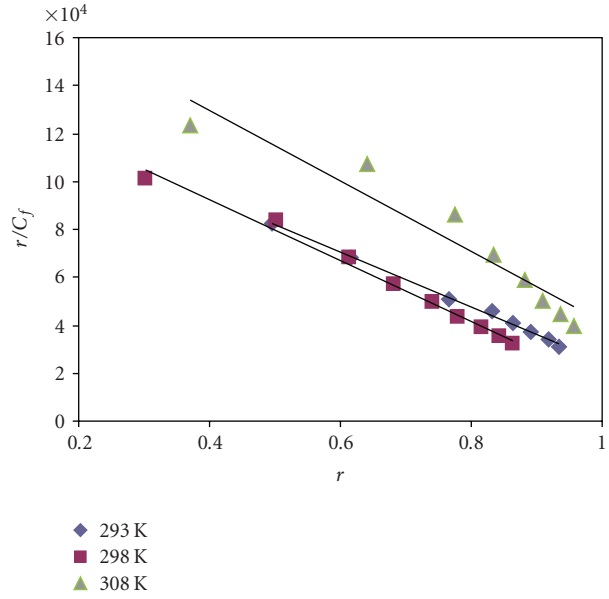

Figure 5: The Scatchard plot for the binding of **1** to HSA.

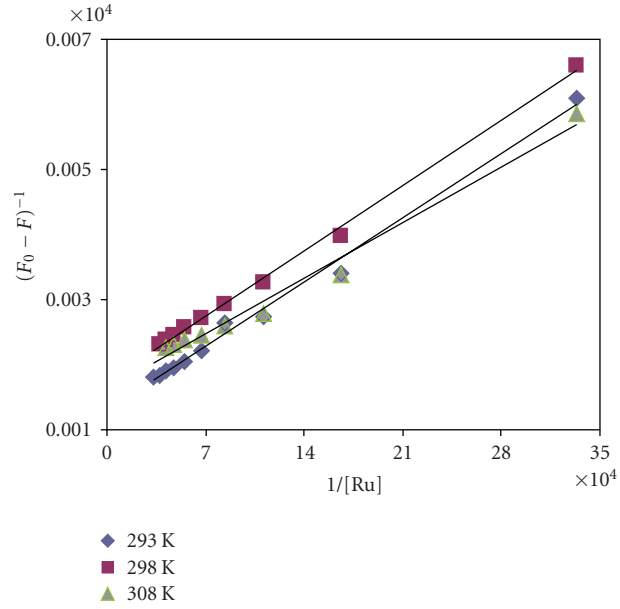

Figure 6: The Linweaver-Burk plot ($1/(F_0 - F)$ versus $1/[\mathrm{Ru}]$) for the reaction of **1** with HSA.

data. The method is based on the following equation:

$$\frac{r}{C_f} = nK + rK, \tag{5}$$

where r is the number of moles of **1** bound per mole of HSA, C_f is the molar concentration of the free metal complex, n is the number of binding sites, and K is the intrinsic binding constant. The analysis (from a plot of r/C_f versus r, Figure 5) suggests that there is a single binding site on the protein as n averages 1.16 over the studied temperature range.

3.2.4. Lineweaver-Burk Analysis. Another method common in the literature for analysis of binding data is the use of the Lineweaver-Burk equation

$$\frac{1}{F_0 - F} = \frac{1}{F_0 K_D [\mathrm{Ru}]} + \frac{1}{F_0}. \tag{6}$$

This equation is somewhat similar to the modified Stern-Volmer equation and a plot of $(F_0 - F)^{-1}$ versus $1/[\mathrm{Ru}]$ (Figure 6) gives K_D the binding constant as the ratio of the intercept to the slope. As seen in Table 1 this method gave similar values for the intrinsic binding constants.

So as Table 1 shows, all the analysis methods gave comparable values for the binding constants. The values of 10^5 are about an order of magnitude greater than for inorganic metal compounds. The complexes $Ni(OAc)_2L_2 \cdot 2H_2O$ and $Cu(OAc)_2L_2 \cdot 2H_2O$ (L = *N*, *N*′-dibenzylethane-1,2-diamine) have binding constants of $1.97 \times 10^4\ M^{-1}$ and $2.36 \times 10^4\ M^{-1}$, respectively [22, 23]. Keppler has reported that Pt(II) complexes of amino alcohols have association constants with HSA ranging from 1.0×10^3 to $2.4 \times 10^4\ M^{-1}$ [23]. The binding constants increase with temperature suggesting that some covalent-type interactions are at play in the binding. The values for f and n (near unity) suggest that the reason for the upward curvature of the Stern-Volmer plot is complex and difficult to elucidate. The quenching could be initiated by the formation of a ground-state complex, but the fact that the binding constants increase with temperature clearly implies that dynamic (collisional) mechanisms play a part in the fluorescence quenching especially at high metal-complex concentrations. This is suggested by Figure 2 as well since the binding site on the protein that was initially exposed to **1** enabled an adduct formation became increasingly buried as more **1** was added.

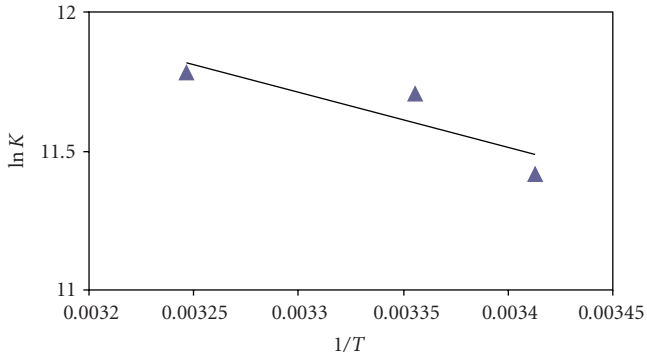

Figure 7: The van't Hoff plot using the equilibrium constants from the modified Stern-Volmer analysis.

Table 2: Thermodynamic parameters for the binding of [(cymene)Ru(ATSC)Cl]PF_6 with the HSA.

Temperature (K)	K^a (10^4 M^{-1})	$\triangle G^\circ$ (kJ/mol)	$\triangle H^\circ$ (kJ/mol)	$\triangle S^\circ$ (J/mol·K)
293	9.09	−28.8		
298	12.1	−29.0	16.7	152
308	13.1	−30.2		

[a]The values of K are from the modified Stern-Volmer analysis.

3.3. Binding Mode Analysis. In protein-ligand binding a number of common intermolecular forces may play significant roles. These include hydrogen-bonding, van der Waals interactions as well as electrostatic and hydrophobic (and other noncovalent) interactions. A thermodynamic analysis, which include determining the enthalpy (ΔH°) and entropy (ΔS°) of reaction, provides insight into the binding mode. The binding constants at various temperatures were used to calculate these parameters using the van't Hoff equation

$$\ln K = \frac{-\Delta H^0}{RT} + \frac{\Delta S^0}{R}, \quad \Delta G^\circ = -RT \ln K. \tag{7}$$

The results from the plot of ln K versus $1/T$ (Figure 7, which is based on the K values from the modified Stern-Volmer analysis) are given in Table 2. The reaction of HSA with 1 is spontaneous as indicated by the negative value for ΔG°. Both ΔH° and ΔS° are positive. In protein-ligand interactions this situation is normally attributed [24] to hydrophobic interactions being the leading contributor to the binding. A positive value for ΔS is also associated with electrostatic interactions and since the metal complex is charged, such interactions cannot be ruled out. The large value of 152 $Jmol^{-1}K^{-1}$ for the entropy change also suggests that the binding process is mostly entropy driven. It might be that as the tryptophan environment changes from a polar (emission maximum near 350 nm) to a more nonpolar state (emission maximum near 325 nm), ordered water molecules are expelled to create a hydrophobic pocket and the entire system becomes more random.

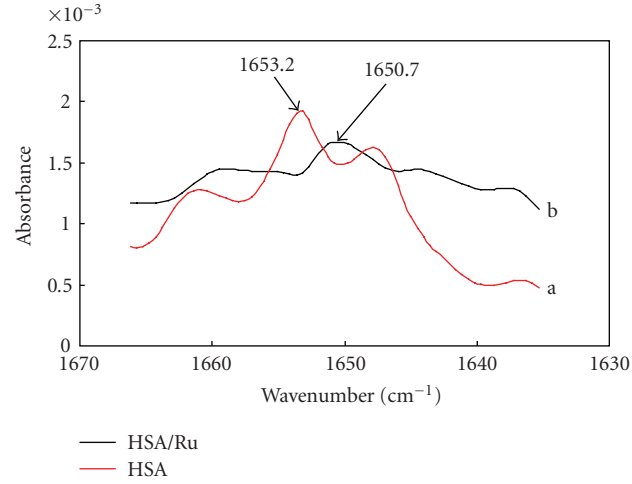

Figure 8: FT-IR spectra of (a) free HSA and (b) the difference spectrum of HSA obtained by subtracting the spectrum of the metal complex from that of the metal complex-HSA solution. [HSA] = [Ru] = 3 μM; 24-hour incubation.

There is no literature precedent for complexes like **1** interacting with HSA, but it is possible that covalent binding to the ruthenium center does occur. The aquation rates for similar compounds are very high (though the rate is dependent on the chelating ligand) and the aquated complexes are generally believed to be more reactive. It is known that DNA binds very strongly (through a guanine residue) to such complexes with the aid of hydrophobic forces [25]. A similar reaction with HSA through the indole ring on the tryptophan would be weak however as it would require deprotonation of the indole nitrogen. By analogy with the purine bases of DNA, this is less probable under physiological pHs. Still, with the data at hand it is not clear that we can quantitatively separate out the contribution of any covalent interaction. Nonetheless this idea is part of the design strategy of this class of anticancer compounds: the incorporation of features that enhance simultaneous hydrophobic and covalent coordination in order to optimize biological targeting.

3.4. Infrared Spectrophotometry. A qualitative assessment of the reaction of **1** with HSA was also undertaken using infrared spectrophotometry. The infrared spectra of proteins exhibit the amide I band (due to stretching of the C=O functional group of the peptide moiety) between 1600 and 1700 cm^{-1}. This band is associated with the secondary structure of the protein [26] and so perturbations of the bond on interaction with the metal compound can provide information on the binding. Figure 7 shows the infrared spectra before and after incubation of HSA with **1**. For a 1 : 1 molar ratio of HSA to **1**, the amide I band shifts position from 1653.2 to 1650.7 cm^{-1}. This indicates that the secondary structure is perturbed noticeably on interaction with **1** and is possibly due to an adduct forming.

4. Conclusion

Organometallic ruthenium compounds are proving to be worthwhile targets as anticancer and antimetastic agents. It is believed that proteins could be the biological target of these compounds and we have shown that compounds with thiosemicarbazone ligands can bind strongly to human serum albumin. Consequently it is fair to suggest that complexes like **1** can be further developed for biological applications.

Acknowledgment

The project described was supported by United States NIH Grant no. P20 RR-16460 from the IDeA Networks of Biomedical Research Excellence (INBRE) Program of the National Center of Research Resources.

References

[1] G. Sava, S. Pacor, A. Bergamo, M. Cocchietto, G. Mestroni, and E. Alessio, "Effects of ruthenium complexes on experimental tumors: irrelevance of cytotoxicity for metastasis inhibition," *Chemico-Biological Interactions*, vol. 95, no. 1-2, pp. 109–126, 1995.

[2] G. Sava and A. Bergamo, "Ruthenium-based compounds and tumour growth control (review)," *International Journal of Oncology*, vol. 17, no. 2, pp. 353–365, 2000.

[3] J. M. Rademaker-Lakhai, D. van den Bongard, D. Pluim, J. H. Beijnen, and J. H. Schellens, "A phase I and pharmacological study with imidazolium-*trans*-DMSO-imidazole-tetrachlororuthenate, a novel ruthenium anticancer agent," *Clinical Cancer Research*, vol. 10, no. 11, pp. 3717–3727, 2004.

[4] G. Sava, R. Gagliardi, A. Bergamo, E. Alessio, and G. Mestroni, "Treatment of metastases of solid mouse tumours by NAMI-A: comparison with cisplatin, cyclophosphamide and dacarbazine," *Anticancer Research*, vol. 19, no. 2, pp. 969–972, 1999.

[5] A. Bergamo, B. Gava, E. Alessio, et al., "Ruthenium-based NAMI-A type complexes with in vivo selective metastasis reduction and in vitro invasion inhibition unrelated to cell cytotoxicity," *International Journal of Oncology*, vol. 21, no. 6, pp. 1331–1338, 2002.

[6] C. G. Hartinger, S. Zorbas-Seifried, M. A. Jakupec, B. Kynast, H. Zorbas, and B. K. Keppler, "From bench to bedside—preclinical and early clinical development of the anticancer agent indazolium *trans*-[tetrachlorobis(1*H*-indazole)ruthenate(III)] (KP1019 or FFC14A)," *Journal of Inorganic Biochemistry*, vol. 100, no. 5-6, pp. 891–904, 2006.

[7] S. Kapitza, M. Pongratz, M. A. Jakupec, et al., "Heterocyclic complexes of ruthenium(III) induce apoptosis in colorectal carcinoma cells," *Journal of Cancer Research and Clinical Oncology*, vol. 131, no. 2, pp. 101–110, 2005.

[8] E. D. Kreuser, B. K. Keppler, W. E. Berdel, A. Piest, and E. Thiel, "Synergistic antitumor interactions between newly synthesized ruthenium complexes and cytokines in human colon carcinoma cell lines," *Seminars in Oncology*, vol. 19, no. 2, supplement 3, pp. 73–81, 1992.

[9] R. E. Morris, R. E. Aird, P. Murdoch, et al., "Inhibition of cancer cell growth by ruthenium(II) arene complexes," *Journal of Medicinal Chemistry*, vol. 44, no. 22, pp. 3616–3621, 2001.

[10] O. Novakova, J. Kasparkova, V. Bursova, et al., "Conformation of DNA modified by monofunctional Ru(II) arene complexes: recognition by DNA binding proteins and repair. Relationship to cytotoxicity," *Chemistry & Biology*, vol. 12, no. 1, pp. 121–129, 2005.

[11] A. Casini, A. Guerri, C. Gabbiani, and L. Messori, "Biophysical characterization of adducts formed between anticancer metallodrugs and selected proteins: new insights from X-ray diffraction and mass spectrometry studies," *Journal of Inorganic Biochemistry*, vol. 108, no. 5-6, pp. 995–1006, 2002.

[12] J. Will, A. Kyas, W. S. Sheldrick, and D. Wolters, "Identification of (η^6-arene)ruthenium(II) protein binding sites in *E. coli* cells by combined multidimensional liquid chromatography and ESI tandem mass spectrometry: specific binding of [(η^6-*p*-cymene)$RuCl_2$(DMSO)] to stress-regulated proteins and to helicases," *Journal of Biological Inorganic Chemistry*, vol. 12, no. 6, pp. 883–894, 2007.

[13] A. Casini, G. Mastrobuoni, M. Terenghi, et al., "Ruthenium anticancer drugs and proteins: a study of the interactions of the ruthenium(III) complex imidazolium *trans*-[tetrachloro(dimethyl sulfoxide)(imidazole)ruthenate(III)] with hen egg white lysozyme and horse heart cytochrome *c*," *Journal of Biological Inorganic Chemistry*, vol. 12, no. 8, pp. 1107–1117, 2007.

[14] A. Casini, C. Gabbiani, E. Michelucci, et al., "Exploring metallodrug-protein interactions by mass spectrometry: comparisons between platinum coordination complexes and an organometallic ruthenium compound," *Journal of Biological Inorganic Chemistry*, vol. 14, no. 5, pp. 761–770, 2009.

[15] P. A. Zunszain, J. Ghuman, T. Komatsu, E. Tsuchida, and S. Curry, "Crystal structural analysis of human serum albumin complexed with hemin and fatty acid," *BMC Structural Biology*, vol. 3, article 6, 2003.

[16] B. Honore, "Conformational changes in human serum albumin induced by ligand binding," *Pharmacology and Toxicology*, vol. 66, supplement 2, pp. 7–26, 1990.

[17] F. A. Beckford, G. Leblanc, J. Thessing, et al., "Organometallic ruthenium complexes with thiosemicarbazone ligands: synthesis, structure and cytotoxicity of [(η^6-*p*-cymene)Ru(NS)CI]$^+$ (NS = 9-anthraldehyde thiosemicarbazones)," *Inorganic Chemistry Communications*, vol. 12, no. 11, pp. 1094–1098, 2009.

[18] S. Krimm and J. Bandekar, "Vibrational spectroscopy and conformation of peptides, polypeptides, and proteins," *Advances in Protein Chemistry*, vol. 38, pp. 181–364, 1986.

[19] J.-S. Mandeville, E. Froehlich, and H. A. Tajmir-Riahi, "Study of curcumin and genistein interactions with human serum albumin," *Journal of Pharmaceutical and Biomedical Analysis*, vol. 49, no. 2, pp. 468–474, 2009.

[20] J. R. Lakowicz and J. G. Weber, "Quenching of fluorescence by oxygen. Probe for structural fluctuations in macromolecules," *Biochemistry*, vol. 12, no. 21, pp. 4161–4170, 1973.

[21] W. R. Ware, "Oxygen quenching of fluorescence in solution: an experimental study of the diffusion process," *The Journal of Physical Chemistry*, vol. 66, no. 3, pp. 455–458, 1962.

[22] S.-S. Wu, W.-B. Yuan, H.-Y. Wang, Q. Zhang, M. Liu, and K.-B. Yu, "Synthesis, crystal structure and interaction with DNA and HSA of (N,*N*′-dibenzylethane-1,2-diamine) transition metal complexes," *Journal of Inorganic Biochemistry*, vol. 102, no. 11, pp. 2026–2034, 2008.

[23] S. S. Aleksenko, C. G. Hartinger, O. Semenova, K. Meelich, A. R. Timerbaev, and B. K. Keppler, "Characterization of

interactions between human serum albumin and tumor-inhibiting amino alcohol platinum(II) complexes using capillary electrophoresis," *Journal of Chromatography A*, vol. 1155, no. 2, pp. 218–221, 2007.

[24] P. D. Ross and S. Subramanian, "Thermodynamics of protein association reactions: forces contributing to stability," *Biochemistry*, vol. 20, no. 11, pp. 3096–3102, 1981.

[25] O. Novakova, H. Chen, O. Vrana, A. Rodger, P. J. Sadler, and V. Brabec, "DNA interactions of monofunctional organometallic ruthenium(II) antitumor complexes in cell-free medial," *Biochemistry*, vol. 42, no. 39, pp. 11544–11554, 2003.

[26] D. M. Byler and H. Susi, "Examination of the secondary structure of proteins by deconvolved FTIR spectra," *Biopolymers*, vol. 25, no. 3, pp. 469–487, 1986.